Activation of Ground Granulated Blast-Furnace Slag by Cement Kiln Dust in Presence of Rice Husk Ash

A. H. Ali[1], Gehad G. Mohamed[2] and Amira A. Elsaman[1]

[1]Housing and Building National Research Centre, Cairo, Egypt
[2]Chemistry Department, Faculty of Science, Cairo University, Cairo, Egypt
amiraelsaman@yahoo.com

Abstract: Blast-furnace slag (BFS) is a finely ground, nonmetallic, rapidly chilled silicate melt material that separated from molten iron in the blast furnace; it consists essentially of glass with crystalline silicates and aluminosilicates of calcium and other cations. The chemical composition of a slag varies considerably depending on the composition of the raw materials in the iron production process. Slag forms shard-like particles that are usually larger than cement grains. This work aims at studying the activation of ground granulated blast-furnace slag (GGBFS) by cement kiln dust (CKD) in the presence of rice husk ash (RHA). GGBFS was replaced by 30 and 50 wt., % CKD. In order to studying the effect of RHA on the consumption of free lime, 5, 7.5 and 10 wt., % RHA were added to the blend containing 50 wt., % CKD. The results showed that, the CKD has a good impact on compressive strength development. The free lime content increases with the increase of CKD %. The results also showed that the RHA has a positive impact on the reduction of free lime content. These facts are confirmed by X-Ray Diffraction (XRD**),** Thermo Gravimetric analysis (TGA) and Differential Thermal analysis (DTA) and scanning electron microscopy (SEM) techniques.
[A. H. Ali, Gehad G. Mohamed and Amira A. Elsaman. **Activation of Ground Granulated Blast-Furnace Slag by Cement Kiln Dust in Presence of Rice Husk Ash.** *Nat Sci* 2016;14(8):123-128]. ISSN 1545-0740 (print); ISSN 2375-7167 (online). http://www.sciencepub.net/nature. 18. doi:10.7537/marsnsj140816.18.

Keywords: GGBFS; CKD; RHA; XRD; Compressive strength

1. Introduction

Portland cement manufacture is considered as one of the most industries which contributes in air pollution. Davidovits[1] stated that one tone of ordinary Portland cement (OPC) generate one tone of CO_2 gas. So, there is a great need for environmentally friendly alternative cement production. Several authors replaced OPC by supplementary cementatious materials (SCMs), in order to minimize the cost and environmental pollution [2-5]. Rice husk ash is categorized as pozzolanic material, which consumes the free lime liberated during OPC hydration [6-9]. SCMs can directly activated by alkaline solution to produce geopolymer cement [10-14]. Alkaline solution is very little and expensive. This study aims at producing economic – activated slag using cement kiln dust as activator.

2.Experimental

2.1. Raw Materials

GGBFS is provided by Iron and Steel Company, Helwan governorate, cement kiln dust (CKD) obtained from El Suize cement company and rice husk is obtained from rice mill, Elmansoura city, then burned at 700 ^{o} C for 2hrs in order to produce rice husk ash (RHA). The chemical composition of the GGBFS, RHA and CKD is shown in Table 1.

2.2. Preparation of Mixes

GGBFS is firstly passed through a 2mm diameter sieve. Also, it is passed through a magnet to remove any contamination of iron melt, then ground in steel ball mill to pass through sieve 45 µm. Different mixes were prepared from GGBFS, CKD and RHA (as addition). The details of dry mix composition are shown in Table (2).

Table 1. Chemical Composition of The GGBFS, RHA and CKD

Oxide contents	GGBFS	RHA	CKD
SiO_2	36.67	71.81	7.44
Al_2O_3	10.31	0.21	2.39
Fe_2O_3	0.50	0.47	2.51
CaO	38.82	1.81	60.40
MgO	1.70	2.10	1.31
Na_2O	0.48	0.19	0.94
K_2O	1.03	8.79	3.95
SO_3	2.17	----	4.18
TiO_2	0.57	----	0.20
P_2O_5	0.04	12.20	0.05
L.O.I	0.12	1.37	11.40
MnO	4.04	0.13	0.11
BaO	3.28	----	----
SrO	0.18	----	---
Cl-	---	----	5.01
Total	99.90	99.89	99.89

Table 2. Composition of The Investigated Mixes, wt%

Mix Notation	GGBFS	RHA	CKD
B50-5	50	5	50
B50-7.5	50	7.5	50
B50-10	50	10	50
B50	50	0	50

2.3.Methods of Investigation

2.3.1. Compressive Strength Determination

At each time interval, compressive strength tests were performed on the hardened pastes using three cubic specimens at each curing time and the average value was recorded as kg/cm^2.Compressive strength of hardened pastes was carried out using five tones German Brüf Pressing Machine with a loading rate of 100 kg/min. The resulting crushed specimens of the hardened pastes were ground and the hydration reaction was stopped.

2.3.2. Free Lime Content (CaO,%)

The free lime content, CaO (%), was determined by using the glycerol/ethanol extraction method and the mean value of the two independent determinations was recorded. It is based on treatment of the hydrated material with hot mixture of absolute dry glycerol and absolute ethyl alcohol.

Free CaO present in the sample will react with dry glycerol with the formation of calcium glycerate. This glycerate is titrated with an alcoholic solution of ammonium acetate. The dried sample (about 0.5 g) was poured in 40 ml of glycerol/ethanol mixture (1: 5 by volume) together with a small amount of anhydrous barium chloride (about 0.5g) as a catalyst, and phenolphthalein as an indicator. The mixture was kept in a conical flask, fitted with an air reflux, heated on a hot plate for 30 minutes (the color becomes pink). The contents of the flask were titrated with a standard alcoholic ammonium acetate solution till the pink color just disappeared. Heating was repeated again and if the pink color reappears, the titration was completed with ammonium acetate solution until no further appearance of pink color occurs upon heating.

3. Results and Discussions

3.1. XRD- Patterns

Figure (1) represents the XRD-patterns of B50-10 mix at 1, 7 and 28 days of curing. It is shown that, the CSH peak intensity increases with time. In contrast, the CH peak intensity decreases with time. This may be explained by the consumption of CH, resulted from the hydration of CaO in CKD, as a result of GGBFS/RHA activation. This is in a good harmony with the results of chemically combined water, free lime, water absorption and compressive strength.

Figure (2) illustrates the XRD-patterns of B50, B50-5, B50-7.5 and B50-10 mixes at 28 days of curing. Clearly, the XRD-pattern of B50-10 mix presents the highest CH peak intensity. This is due to the reaction between CH and amorphous silica in RHA, forming CSH in GGBFS-CKD matrix. The peak intensity at ~ 29.45 2θ decreases with the addition of RHA. This may be attributed to that the possibility of atmospheric carbonation decreases with RHA content.

3.2. Thermogravimetric Analysis

Figure (3a&b) displays the TG & DTG – thermograms of B50-10 mix at 1,7 and 28 days. Obviously, the weight loss and endothermic peak intensity around 450 °C decrease with time. This is due to the continuous activation of GGBFS/RHA hydration by CH with the increase of time. In contrast, the weight loss and endothermic peak intensity in range of 70-200 °C increase with time, suggesting the successive CSH and CASH hydration products with the increase of curing time. The TG/DTG analysis is in a good agreement with compressive strength results.

Fig. (4a&b) show the TG/DTG thermograms of CKD-GGBFS blend (B50) containing 0, 5, 7.5 and 10 wt, % RHA at 28 days. Obviously, as the amount of RHA increases the weight loss increases. This is due to the successive CSH formation with RHA content. The CH endothermic peak intensity decreases with the increase of RHA, %. This confirms a good pozzolanicreactivity of RHA.

3.3. Compressive Strength

Figure (5) shows the compressive strength of B50, B50-5, B50-7.5 and B50-10 mixes. The addition of RHA has a positive effect on the compressive strength development. The higher the RHA content, the higher the compressive strength values at all ages. It is clear that the addition of 5, 7.5 and10% of RHA leads to increase the compressive strength value by~ 5, 13 and 18%, respectively as compared with control sample (with no RHA) at 90 days of curing. This proved that the free lime consumption enhancement with RHA, leading to the formation of excessive CSH content.

3.4. Free Lime Contents (Cao%)

Figure (6) shows the free lime content of B50, B50-5, B50-7.5 and B50-10 mixes. A noticeable decrease in the free lime values have been observed in all mixes containing different proportion of RHA at all ages of hydration from 1 up to 90 days. This fact should be related to the consumption of free lime by the interaction with active silica in RHA forming CSH. Besides, the addition of 5, 7.5 and 10 % RHA leads to decrease the free lime content by ~ 45.49, 55.04 and 67.16 %, respectively as compared with the control sample (B50) after 90 days of curing.

3.5.Scanning Electron Microscopy (SEM)

Figure (7) shows the SEM- photos of B50-10 mix at 1 and 28 days. The microstructure at 1 day is less ordered than that of at 28 days. This is due to the

RHA has a low hydration rate at early ages of curing, causing the formation of silica gel, which coat slag grains and therefore, decrease its hydration rate. The RHA needle can be observed in the microstructure at 1 day and disappeared at 28 days. This is due to the continues of RHA hydration and its reaction with free lime, forming additional CSH content in the matrix.

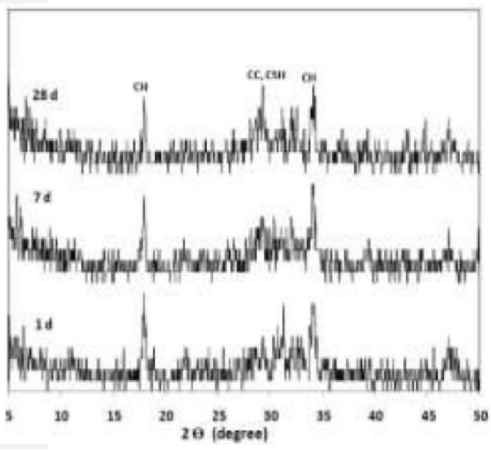

Fig. (1): XRD-Patterns of B50-10 at 1, 7 and 28 days

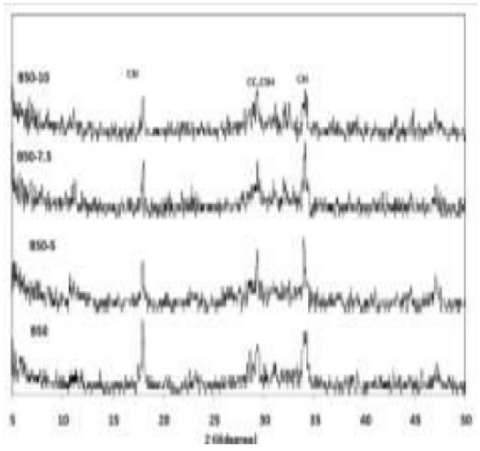

Fig. (2): XRD Patterns of B50, B50-5, B50- 7.5 and B50-10 at 28 days

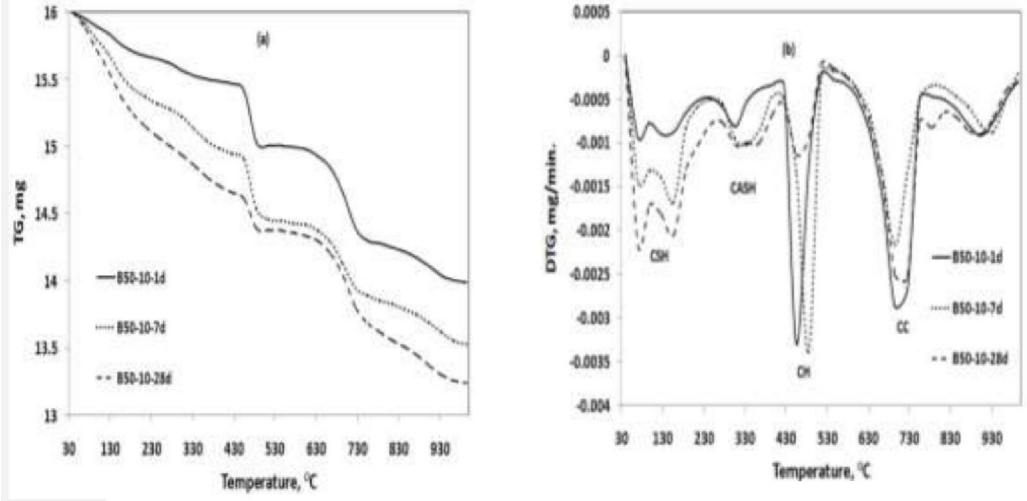

Fig. (3): (a)TG and (b) DTG-Thermograms of B50-10 Mix at 1, 7 and 28 Days

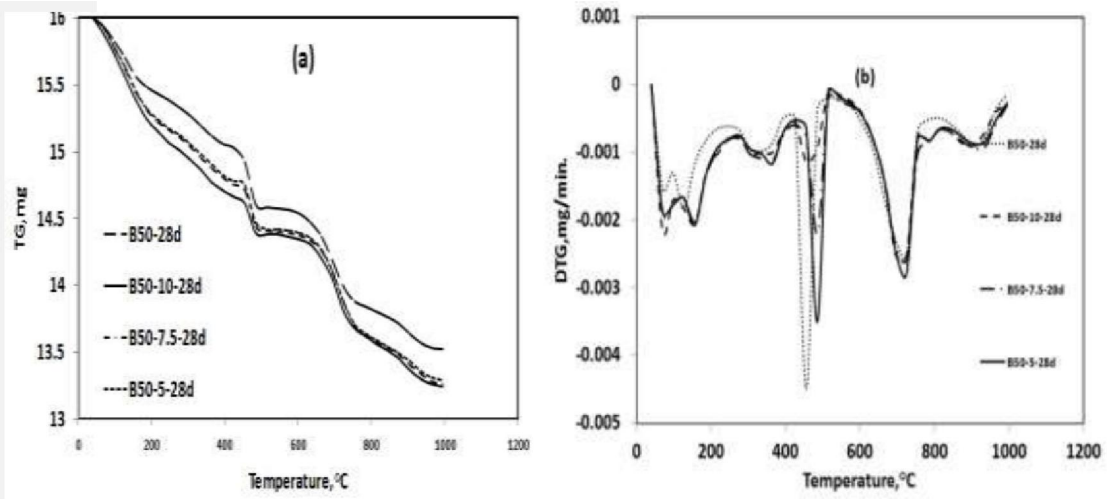

Fig. (4): (a) TG and (b) DTG-Thermograms of B50, B50-5, B50-7.5 andB50-10 at 28 days

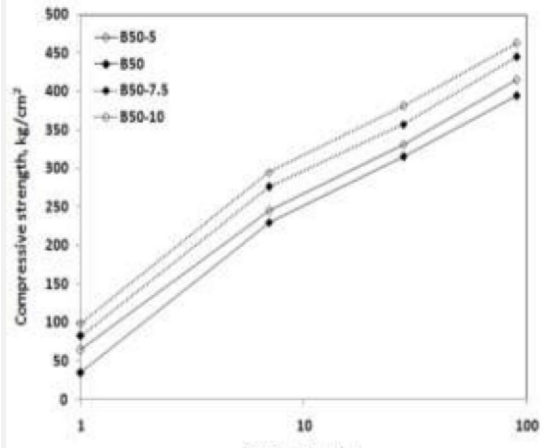

Fig (5): Compressive strength of GGBFS-CKD-RHA mixes

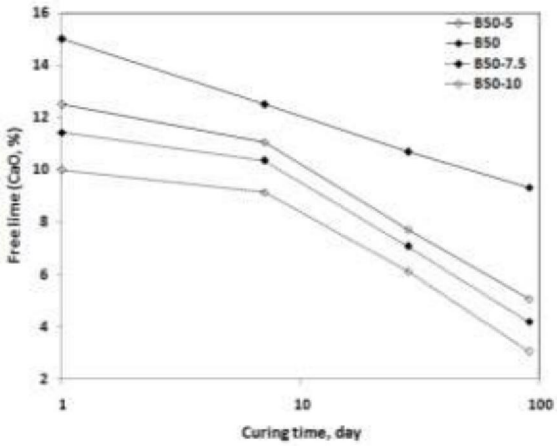

Fig (6): Fee lime of GGBFS-CKD-RHAmixes

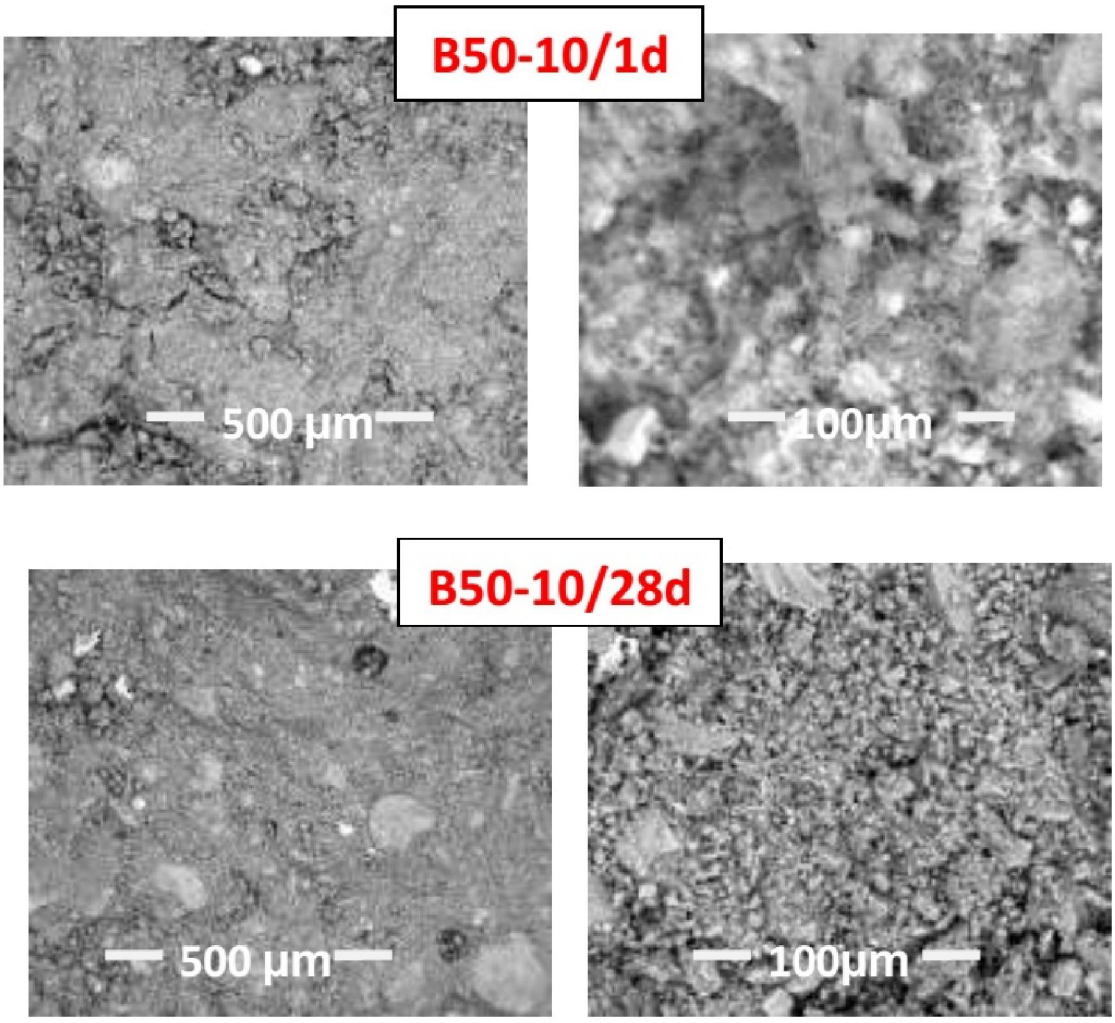

Fig. (7) Shows the SEM- Photos of B50-10 Mix at 1 and 28 Days

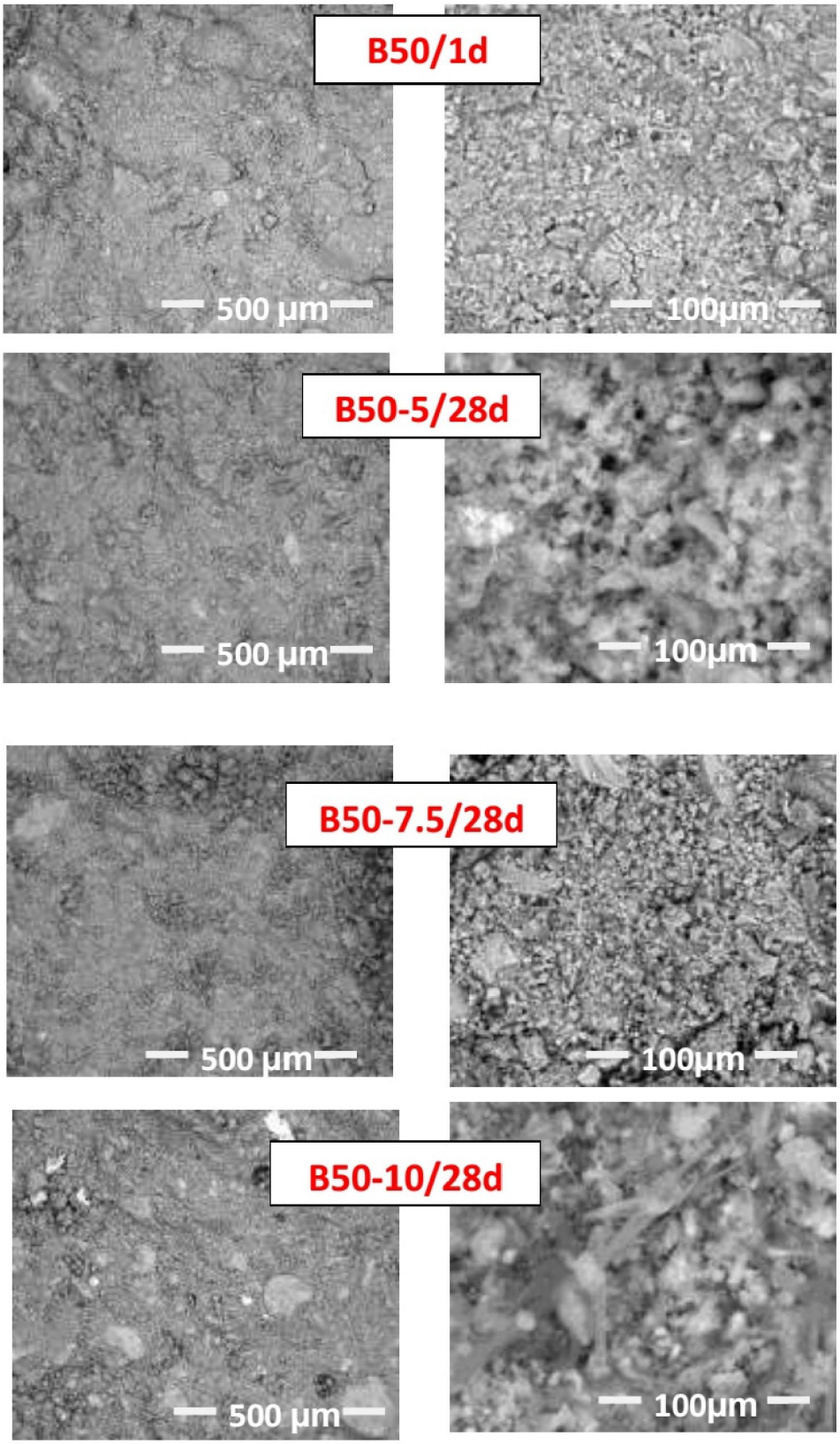

Fig. (8): SEM- Photographs of B50, B50-5, B50-7.5 and B50-10 at 28 days

Figure (8) shows the SEM- photographs of B50, B50-5, B50-7.5 and B50-10 mixes at 28 days of curing. The compaction of microstructure enhances in direction of B50-10 > B50-7.5 > B50-5> B50. This is mainly due to the formation of additional CSH content in the matrix resulted from the reaction between RHA and free lime. The needle crystal can be observed in B50-10 microstructure, meaning that all free lime has been consumed by RHA.

4. Conclusion

Several findings can be concluded as follows:

1-The free lime increase with the increase of CKD contents.

2-The compressive strength increases with CKD content.

3-The addition of RHA has a good impact on mechanical properties of GGBFS-CKD blends.

4-The XRD, TG/DTG and SEM confirmed that CKD induce the GGBFS hydration. Also, confirmed the positive impact of RHA on the compressive strength development and free lime consumption.

References

1. Davidovits, J. Geopolymer chemistry and applications, the manufacture of geopolymer cement 2011 paris; 3rd ed: 533 -560.
2. Jun Zhang, Qing Wang, Zhenbo Wang. Optimizing design of high strength cement matrix with supplementary cementitious materials. Construction and Building Materials 2016; 120: 123–136.
3. Romy S. Edwin, Mieke De Schepper, Elke Gruyaerta, Nele De Belie. Effect of secondary copper slag as cementitious material in ultra-high performance mortar.Construction and Building Materials 2016; 119: 31–44.
4. Reza Saleh Ahari, Tahir Kemal Erdem, Kambiz Ramyar. Thixotropy and structural breakdown properties of self-consolidating concrete containing various supplementary cementitious materials. Cement and Concrete Composites 2015; 59: 26–37.
5. Adorján Borosnyói. Long term durability performance and mechanical properties of high performance concretes with combined use of supplementary cementing materials. Construction and Building Materials 2016; 112:307–324.
6. Lech W.O. Soares, Renata M. Braga, Julio C.O. Freitas, Rafael A. Ventura, Dennys S.S. Pereira, Dulce M.A. Melo. The effect of rice husk ash as pozzolan in addition to cement Portland class G for oil well cementing, Journal of Petroleum Science and Engineering 2016;131: 80–85.
7. Ehsan Mohseni, Farzad Naseri, Ramin Amjadi, Mojdeh Mehrinejad Khotbehsara, Malek Mohammad Ranjbar. Microstructure and durability properties of cement mortars containing nano-TiO2 and rice husk ash. Construction and Building Materials2016 ; 114:656–664.
8. Rêgo J.H.S., A.A. Nepomuceno, E.P. Figueiredo, N.P. Hasparyk, Microstructure of cement pastes with residual rice husk ash of low amorphous silica content. Construction and Building Materials 2015 ; 80: 56–68.
9. Mahboubeh Zahedi, Ali Akbar Ramezanianpour, Amir Mohammad Ramezanianpour. Evaluation of the mechanical properties and durability of cement mortars containing nanosilica and rice husk ash under chloride ion penetration, Construction and Building Materials2015; 78:354–361.
10. Vilaplana J.L., F.J. Baeza, O. Galao, E.G. Alcocel, E. Zornoza, P. Garcés. Mechanical properties of alkali activated blast furnace slag pastes reinforced with carbon fibers. Construction and Building Materials 2016 ;116: 63–71.
11. Yiquan Liu, Weiping Zhu, En-Hua Yang. Alkali-activated ground granulated blast-furnace slag incorporating incinerator fly ash as a potential binder. Construction and Building Materials 2016; 112:1005–1012.
12. Paulo H.R. Borges, Nemkumar Banthia, Himad A. Alcamand, Wander L. Vasconcelos, Eduardo H.M. Nunes. Performance of blended metakaolin/blastfurnace slag alkali-activated mortars. Cement and Concrete Composites2016 ; 71: 42–52.
13. Jin Wang, Jun-xia Wang, Qin Zhang, Yu-xiang Li. Immobilization of simulated low and intermediate level waste in alkali-activated slag-fly ash-metakaolinhydroceramics. Nuclear Engineering and Design2016; 300: 67–73.
14. Gao X., Q.L. Yu, H.J.H. Brouwers. Assessing the porosity and shrinkage of alkali activated slag-fly ash composites designed applying a packing model. Construction and Building Materials 2016;119: 175–184.

8/10/2016